Catecholaminergic neuromodulation and selective attention jointly shape perceptual decision making

S.A. Nuiten[a,b*], J.W. De Gee[b,c,d,e], J.J. Fahrenfort[a,b,f,g], S. van Gaal[a,b*]

a. Department of Psychology, University of Amsterdam, Amsterdam, NLD;

b. Amsterdam Brain & Cognition, University of Amsterdam, Amsterdam, NLD;

c. Department of Neuroscience, Baylor College of Medicine, Houston, USA;

d. Jan and Dan Duncan Neurological Research Institute, Texas Children's Hospital, Houston, USA;

e. Cognitive and Systems Neuroscience, Swammerdam Institute for Life Sciences, University of Amsterdam, Amsterdam, NLD;

f. Institute for Brain and Behavior Amsterdam, Vrije Universiteit Amsterdam, Amsterdam, NLD;

g. Department of Experimental and Applied Psychology - Cognitive Psychology, Vrije Universiteit Amsterdam, Amsterdam, NLD

*Corresponding authors

Funding

This research was supported by an ERC starting grant from the H2020 European Research Council (ERC STG 715605 to S.v.G).

Author contributions

S.A.N. and S.v.G. designed research; S.A.N. collected data; S.A.N. and J.W.G. analyzed the data; S.A.N. and S.v.G. wrote the first draft of the paper; J.W.G. and J.J.F. edited the paper.

Abstract

Perception of sensory input is influenced by fluctuations in ongoing neural activity, most prominently driven by attention and neuromodulator systems. It is currently unknown if neuromodulator activity and attention differentially modulate neural activity and perception or whether neuromodulatory systems in fact control attentional processes. We pharmacologically enhanced cholinergic (through donepezil) and catecholaminergic (through atomoxetine) levels in humans performing a visual attention task to investigate the effects of neuromodulatory drive and spatial attention on neural activity and behavior. Attention and catecholaminergic enhancement both improved perceptual sensitivity by increasing the rate of evidence accumulation towards a decision threshold (cholinergic effects were negligible). Electroencephalographic recordings revealed that attention and catecholaminergic enhancement both modulated pre-stimulus cortical excitability, evoked sensory processes and parietal evidence accumulation. Crucially however, the spatial profile and timing of these effects were remarkably different. This suggests that selective attention and neuromodulatory systems shape perception largely independently and in qualitatively different ways.

Introduction

Agents often make inconsistent and varying decisions when faced with identical repetitions of (sensory) evidence[1–3]. Recent laboratory experiments, meticulously controlling for external factors, have shown that ongoing fluctuations in neural activity may underlie such behavioral variability[4]. Variability in behavioral responses, however, is not exclusively related to alterations in the decision-making process, but may in fact find its root cause in fluctuations in (conscious) perception leading up towards the decision[5–9].

Candidate sources of these fluctuations in cortical activity and behavior are systematic variations in attention and central arousal state[10,11]. Attention to – and predictions about – specific features of sensory input (e.g. its spatial location or content) results in facilitated processing of this input and is associated with improved behavioral performance[12,13]. The central arousal state of animals is controlled by the activity of neuromodulators, including noradrenaline (NA)[14] and acetylcholine (ACh)[15,16], which globally innervate cortex. Contrary to attention, the relation between neuromodulator activity and behavioral performance is non-monotonic, with optimal behavioral performance occurring at intermediate levels of neuromodulation[14,17].It is currently unknown if fluctuations in attention and neuromodulator activity contribute to neural and behavioral variability in the same way. Both attention and neuromodulators can alter the input/output ratio (or: gain) of single neurons and neuronal networks, thereby modulating the impact of (sensory) input on cortical processing[14,18,19] and thus possibly perceptual experience. For example, recordings in macaque middle temporal area (MT) have provided evidence for attentional modulation of neural gain, by showing increased firing rates for neurons having their receptive field on an attended location in space, but suppressed firing rates for neurons with receptive fields outside that focus, under identical sensory input[20]. Likewise, both noradrenaline and acetylcholine are known to modulate firing rates of neurons in sensory cortices[16]. To illustrate, the arousal state of mice, driven by neuromodulator activity, strongly modulates ongoing membrane potentials in auditory cortex and as such can shape optimal states for auditory detection behavior[17]. Neuromodulator activity and attention also have similar

effects on network dynamics, as both increase cortical desynchronization and enhance the encoding of sensory information[10,21]. These similar neural effects of attention and neuromodulators have raised the question whether neuromodulatory systems control (certain aspects of) attention[21].

Here, we addressed this question by investigating if and how covert spatial attention and neuromodulatory systems jointly shape, in isolation and in interaction, visual perception in humans. To test this, we pharmacologically enhanced the tonic (baseline) level of catecholamines (noradrenaline and dopamine, through atomoxetine) and acetylcholine (through donepezil) in human participants performing a probabilistic attentional cueing task, while we measured electroencephalography (EEG) and pupillary responses. Participants reported the orientation of a briefly presented Gabor patch, presented left or right of fixation, as being clockwise (CW; 45°) or counterclockwise (CCW; -45°). A visual cue predicted the location of the Gabor with 80% validity (the cue did not predict orientation, see **Figure 1A**). This set-up allowed us to test the effects of increased neuromodulator levels (drug effects) and spatial attention (cue validity effects) on several stages of cortical processing leading up to the perceptual decision about Gabor orientation. We characterized the effects of drug condition and cue validity on I) perceptual sensitivity (derived from signal detection theory[22]), II) latent decision parameters, derived from drift diffusion modeling[23], III) accumulation of sensory evidence over time towards a decision[24–26], IV) stimulus-evoked activity[26–28], and (V) pre-stimulus cortical excitability[29,30].

Results

Catecholaminergic enhancement increases physiological markers of bodily arousal

We employed a randomized, double-blind crossover design in which atomoxetine (ATX, 40mg), donepezil (DNP, 5mg) and placebo (PLC) were administered in different EEG recording sessions (drug order was counterbalanced between participants, **Figure 1B**). ATX is a relatively selective noradrenaline reuptake inhibitor, which inhibits the presynaptic noradrenaline reuptake transporter, thereby resulting in increased NA and dopamine (DA) levels[31]. DNP is a cholinesterase inhibitor, which impedes the breakdown of acetylcholine by cholinesterase, thereby resulting in overall increased acetylcholine levels[32]. Participants received two pills on each recording session, the order of which depended on the specific drug session (**Figure 1C**, for more details on drug administration see **Methods**).

To gauge the effect of our pharmaceuticals, we collected physiological and subjective state measures at different moments throughout the day (from 9:00 – 16:00; **Figure 1D-1J**; for details see **Methods** and **Supplementary Information**). Ingestion of ATX resulted in several physiological responses associated with higher states of arousal, including increased heart rate and blood pressure, at the start of the behavioral experiment (**Figure 1D-1J**, **Supplementary Information**), in line with previous non-clinical reports[33,34]. We did not observe any physiological effects of DNP (**Figure 1D-1J**, **Supplementary Information**), which, to our knowledge, have not been reported in previous studies either[33–36].

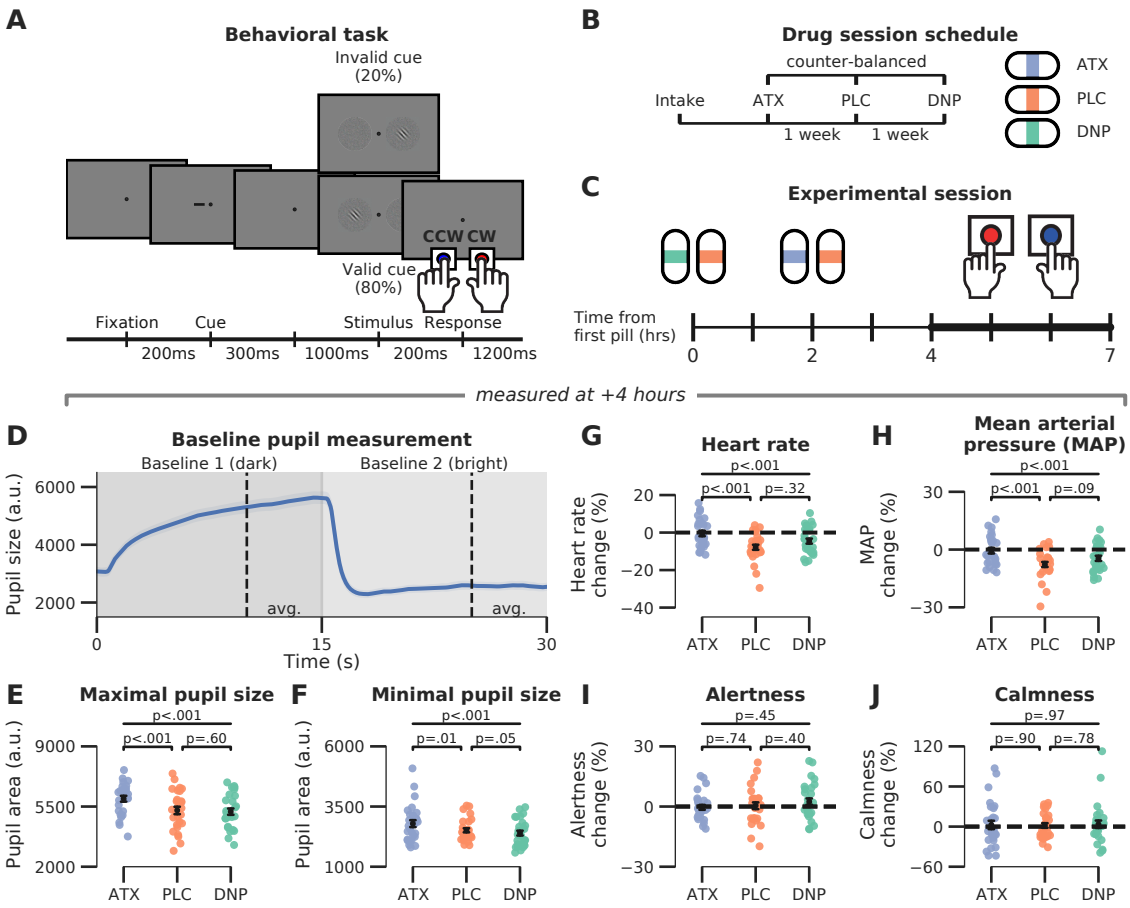

Figure 1. Experimental setup: behavioral task, pharmacological manipulation and physiological responses. A) Schematic representation of the behavioral task. Participants responded to the orientation (CW/CCW) of unilaterally presented Gabor stimuli that were embedded in noise (bilaterally presented). The likely location of the Gabor stimulus was cued (horizontal dash presented 0.33° left/right from fixation) with 80% validity before stimulus onset. **B)** Schematic overview of experimental sessions. Participants came to the lab on four occasions: one intake session and three experimental sessions. On the experimental sessions, participants received either placebo (PLC, data in orange), donepezil (DNP, 5mg, data in green) or atomoxetine (ATX, 40mg, data in blue). Drug order was counterbalanced across participants. **C)** Time schedule of experimental sessions. Participants received a pill on two moments in each session, one at the beginning of the session and a second pill two hours later. The first pill contained either placebo (PLC and ATX session) or donepezil (DNP session), the second pill was either a placebo (PLC and DNP session) or atomoxetine (ATX session). Behavioral testing started 4 hours after administration of the first pill. **D)** Baseline pupil diameter was measured before onset of the behavioral task. Participants fixated while the background luminance of the monitor was dimmed (for 15s) and then brightened (for 15s) to establish the pupil size in dark and bright circumstances. **E)** Pupil diameter during the dark (left) and bright (right) measurement windows for each drug condition separately. **G-H)** Effects of drug on heart rate (panel **G**) and mean arterial blood pressure (MAP; panel **H**, see **Methods**). Measurements were baseline-corrected to the first measurement taken right before ingestion of the first pill. **I-J)** Effects of drug on subjective ratings of alertness (panel **I**) and (panel **J**) calmness, derived from Visual Analogue Scale (VAS, see **Methods**). *Abbr.*: ATX: atomoxetine, PLC: placebo, DNP: donepezil

Catecholaminergic enhancement improves the sensitivity of perceptual decisions

We first report the effects of cue validity and drug on perceptual sensitivity (d'), derived from Signal Detection Theory (SDT)[22], and reaction times (RT) with 3x2 (drug x attention) repeated measures (rm)ANOVAs and 2x2

factor (drug x cue validity) rmANOVAs pairwise drug comparisons (drug vs. placebo, see **Methods** for detailed description of statistical analyses).

Although the overall main effect of drug on d' was not robust ($F_{2,54}$=2.80, p=.07, η_p^2=0.09; **Figure 2A**), post-hoc t-tests indicated that d' was improved by ATX, but not by DNP, compared to PLC (ATX: $F_{1,27}$=4.28, p=.048, η_p^2=0.14; DNP: $F_{1,27}$=1.61, p=.22, η_p^2=0.06, BF_{01}=1.58; **Figure 2A**). RTs were not affected by drug ($F_{2,54}$=1.33, p=.27, η_p^2=0.05, BF_{01}=1.99; **Figure 2B**), and pairwise comparisons (vs. PLC) were also not significant for neither ATX nor DNP (ATX: $F_{1,27}$=1.39, p=.25, η_p^2=0.05, BF_{01}=1.59; DNP: $F_{1,27}$=2.82, p=.11, η_p^2=0.10, BF_{01}=0.95). As expected, validly cued (attended) targets were associated with improved d' and increased response speed compared to invalidly cued (unattended) targets (d': $F_{1,27}$=39.22, p<.001, η_p^2=0.59; RT: $F_{1,27}$=43.47, p<.001, η_p^2=0.62). This beneficial effect of cue validity on d' was not modulated by drug ($F_{2,54}$=2.11, p=.13, η_p^2=0.07. BF_{01}=1.87; **Figure 2B**), although post-hoc tests showed a trending interaction between cue validity and ATX ($F_{1,27}$=3.76, p=.06, η_p^2=0.12), but not DNP ($F_{1,27}$=1.61, p=.22, η_p^2=0.06, BF_{01}=2.00). The beneficial effect of cue validity on RT was not modulated by drug ($F_{2,54}$=1.35, p=.27, η_p^2=0.05, BF_{01}=3.33). Participants did not exhibit biased decision making across all conditions (SDT criterion, one-sample two-sided t-test against zero; t(27)=-0.61, p=.55, d=0.11, BF_{01}=4.19; **Supplementary Figure S2**), nor did we observe robust effects of drug and/or cue validity on overall decision bias (**Supplementary Figure S2**). However, absolute (unsigned) bias was decreased for validly cued targets, indicating that the subject-specific bias is diminished when the Gabor location was validly cued (**Supplementary Figure S2**). We did not observe effects of cue validity or drug on choice history bias[37] (**Supplementary Figure S2)**.

Drift diffusion modelling: ATX and spatial attention enhance rate of sensory evidence accumulation

We next fitted a drift-diffusion model (DDM) to the behavioral data to gain a better understanding of the effects of drug and cue validity on latent variables of decision formation[23]. The DDM describes perceptual decisions as a noisy accumulation process of evidence over time that is terminated when accumulated evidence crosses a certain decision threshold (**Figure 2C**). Based on previous literature, we hypothesized that cue validity would mainly affect sensory evidence accumulation reflected in drift rate (v)[28,38], further suggested by the fact that valid cues resulted in better and faster performance on Gabor discrimination (**Figure 2A,B**). On the contrary, although performance improved under ATX, average RTs were not affected, suggesting that other parameters may also have been modulated by drug besides drift rate. So, to tease apart the effects of cue validity and drug condition, we fitted a model in which drift rate, boundary separation (b) and non-decision time (t_0) were allowed to fluctuate with cue validity and drug. We included drift rate variability to account for between trial variance in drift rate. We fitted two hierarchical Bayesian regression models to capture within-subject effects of both drug and cue validity: one for ATX vs. PLC and one for DNP vs. PLC. Note that these regression models did not allow to include all three drug conditions in one model and therefore this is the only analysis in which we applied a 2x2 factorial design (drug x cue validity) for both ATX and DNP separately. The Bayesian implementation of the DDM constrained single-subject parameter estimates on the basis of group-level parameter distributions. Model fits are reported in **Supplementary Figure S3**.

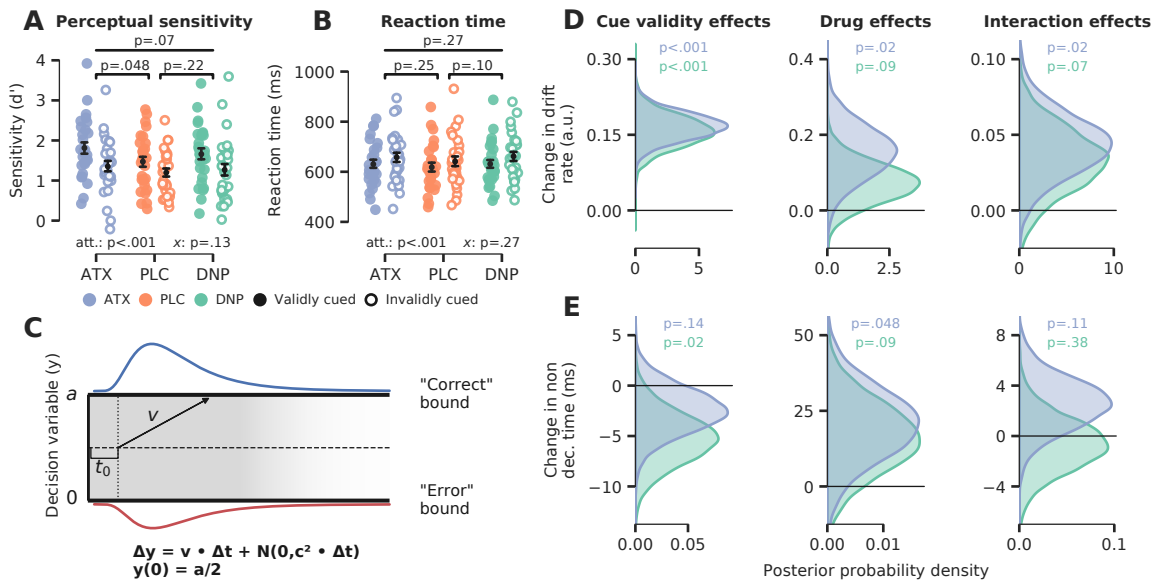

Fig. 2 Behavioral results. A) Signal detection theoretic sensitivity (d'), separately per drug and cue validity. **B)** As A, but for reaction time (RT). **C)** Schematic of the drift diffusion model (DDM), accounting for behavioral performance and reaction times. The model describes behavior on the basis of various latent parameters, including drift rate (*v*), boundary separation (*a*) and non-decision time (t_0). **D-E)** As A, but for drift rate and non-decision time separately for the three drug conditions.

First, we indeed found that validly cued trials were associated with increased drift rates (both models p<.001; **Figure 2D**). We also observed increased drift rate under ATX, but not DNP (ATX model: p=.02, DNP model: p=.09; **Figure 2D**). Moreover, ATX increased the effects of cue validity on drift rate, but DNP did not (ATX model: p=.02, DNP model: p=.07; **Figure 2D**). Although the rate of evidence accumulation was increased under ATX, the onset of this accumulation was delayed, indexed by an increase in non-decision time (ATX model: p=.04, DNP model: p=.07; **Figure 2E**). The effect of cue validity on non-decision time was not robust, when taking both models into account (ATX model: p=.15, DNP model: p=.02; **Figure 2E**). We also did not observe any interaction effects between cue validity and drug on non-decision time (ATX model: p=.07, DNP model: p=.45; **Figure 2E**). Cue validity and drug did not affect decision bound separation, showing that response caution was not under the influence of neuromodulation or attention (**Supplementary Figure S4**). We fitted two additional models (for ATX and DNP vs. PLC) that allowed drift rate variability to also fluctuate with cue validity and drug, while keeping decision bound fixed. We used this model to test whether these effects were indeed related to overall drift rate and not drift rate variability[39]. We observed no effects of cue validity and drug on drift rate variability showing that the overall rate, and not the consistency, of evidence accumulation was enhanced by drug and cue validity (**Supplementary Figure S6**).

Neuromodulatory changes in evidence accumulation reflected in centro-parietal accumulation signal

Recently, a positively trending signal over centro-parietal cortex was identified as a neural marker reflecting evidence accumulation in perceptual decision tasks. This component, termed the centro-parietal positivity (CPP), has been shown to track task difficulty, RTs, and task performance during challenging perceptual decisions[38,40]. The CPP furthermore scales independently of stimulus identity (unsigned component, identical for two or more

stimulus categories), correlates with drift rate as derived from modelling behavior with DDMs and as such is regarded as a neural reflection of the decision variable (i.e. accumulated evidence, **Figure 2C**)[41].

We plotted the CPP locked to the response in **Figure 3.** In line with previous studies[38,40], the CPP predicted the accuracy and speed of perceptual decisions: CPP amplitude at the time of the response and its slope in the time-window starting -250ms preceding the response were both higher for correct than erroneous decisions (amplitude: t(27)=5.86, p<.001, d=0.49; slope: t(27)=5.76, p<.001, d=0.46; **Figure 3A**), whereas decision speed was uniquely associated with CPP slope (amplitude: t(27)=1.44, p=.16, d=0.14, BF_{01}=1.99; slope: t(27)=3.19, p=.004, d=0.51; **Figure 3B**). Moreover, subjects with high drift rate (across all conditions, median split) showed both higher CPP amplitude and slope (independent t-test; amplitude: t(26)=2.61, p=.01, d=0.99; slope: t(26)=2.24, p=.03, d=0.85; **Figure 3C**), indicating that the CPP indeed reflects accumulated evidence over time[40,41].

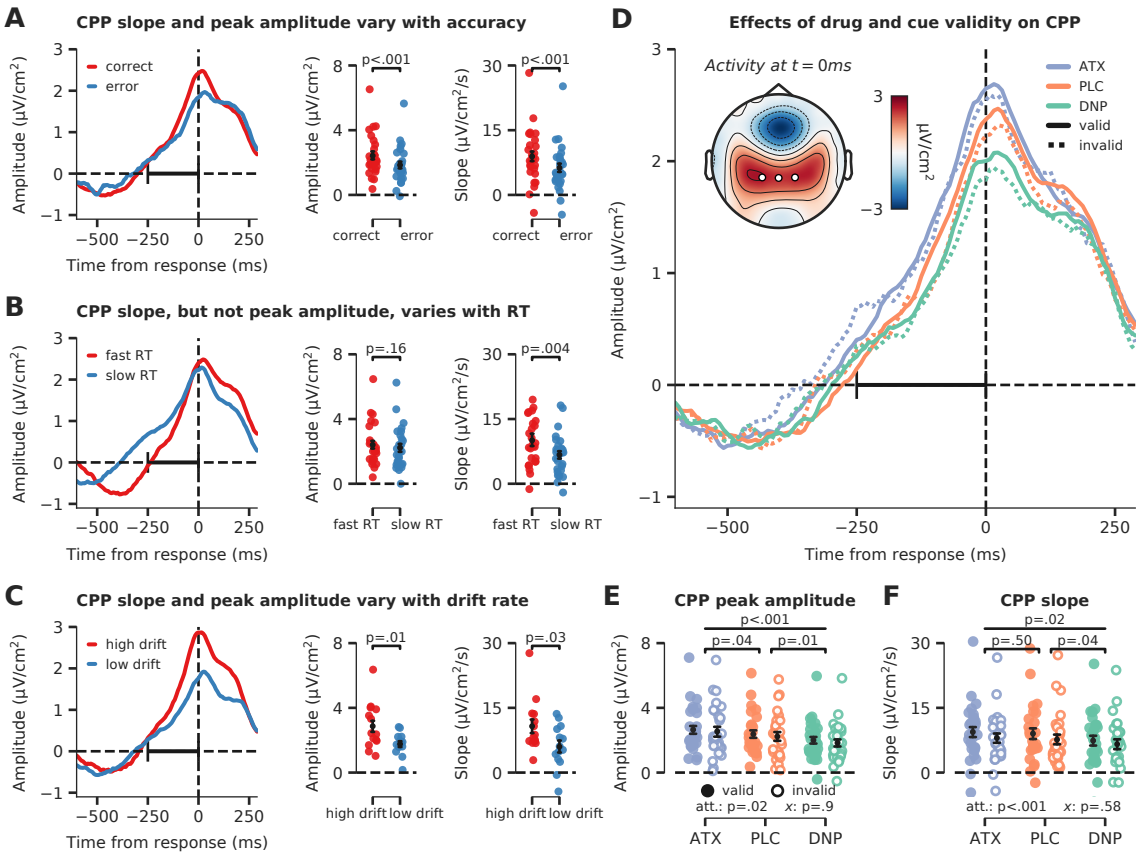

Figure 3. Evidence accumulation is affected by cue validity and drug, indexed by changes in centroparietal positivity (CPP). A) Response-locked CPP for correct and incorrect answers, **B)** for trials with fast and slow RTs and **C)** for participants with overall high drift rate. **D)** Modulation of response-locked CPP by drug and cue validity. The horizontal black line indicates the time-window for which CPP slope was calculated (linear regression from -250ms to 0ms pre-response). The topographic map shows activation at the moment of the response, with white markers indicating the centro-parietal ROI used for the CPP analyses (channels CP1, CP2, CPz). **E)** Peak CPP amplitude, separately for drug and cue validity. **F)** CPP slope for all drug and cue validity conditions.

After establishing the CPP as a reliable marker of evidence accumulation, we inspected its relation to neuromodulatory drive and cue validity (**Figure 3D**). Interestingly, drug condition affected the amplitude and

192 slope of the CPP (main effects of drug, amplitude: $F_{2,54}$=10.67, p<.001, η_p^2=0.28, **Figure 3E**; slope: $F_{2,54}$=4.31, p=.02,
193 η_p^2=0.14, **Figure 3F**). Specifically, CPP amplitude was heightened by ATX compared to PLC (amplitude: t(27)=2.17,
194 p=.04, d=0.21; slope: t(27)=0.66, p=.51, d=0.06, BF_{01}=4.08), whereas DNP lowered CPP peak amplitude and
195 decreased its slope compared to PLC (amplitude: t(27)=-2.88, p=.01, d=0.31; slope: t(27)=-2.24, p=.03, d=0.22).

196 Trials on which target locations were validly cued were associated with an increased CPP slope, whereas
197 amplitude modulations were less robust (amplitude: $F_{1,27}$=3.97, p=.06, η_p^2=0.13, **Figure 3E**; slope: $F_{1,27}$=13.61,
198 p=.001, η_p^2=0.34, **Figure 3F**). Drug condition and cue validity shaped CPP slope and peak amplitude
199 independently, because no interaction effects were observed (amplitude: $F_{2,54}$=0.19, p=.82, η_p^2=0.01, BF_{01}=8.47,
200 **Figure 3E**; slope: $F_{2,54}$=0.43, p=.65, η_p^2=0.02, BF_{01}=6.90, **Figure 3F**). Summarizing, we show that drug condition and
201 cue validity both affect the CPP, but they do so by affecting different features of this component (i.e. peak
202 amplitude and slope, respectively).

203 **Stimulus-locked signals over occipito-temporal sites precede evidence accumulation and are modulated**
204 **by catecholaminergic stimulation and attention**

205 Previous studies investigating the neural origins of perceptual decision-making during visual tasks have observed
206 early EEG deflections at lateral occipito-temporal sites that reflect target selection prior to CPP build-up[26,28].
207 These target related signals in perceptual decision tasks are usually measured at electrode sites P7/P9 (left
208 hemifield) and P8/P10 (right hemifield) and are referred to as the N2c (contralateral to the target) and N2i
209 (ipsilateral to the target)[24,26]. They form the basis of the N2pc component, which is derived by subtracting them
210 and is often explored in visual search paradigms[27,42]. Similar to the CPP, N2c amplitude scales with RT and
211 stimulus coherence and shifts in its peak latency have been shown to influence the onset of the CPP[28].

212 We performed a cluster corrected 3x2x2 factorial (drug x target location x cue direction) rmANOVA across time
213 to test for effects of spatial attention (difference in activity between regions contralateral vs. ipsilateral to the
214 spatial cue), target selection (difference in activity between regions contralateral vs. ipsilateral to the target),
215 and drug condition, as well as possible interaction effects on stimulus-locked occipito-temporal activity. To
216 anticipate the results, we only observed main effects of each of the three factors and no interactions. Because
217 of the large number of EEG traces to plot and compare (12 in total) we first focus on overall effects of cue
218 direction and drug condition, thereby collapsing over target location. Thereafter we will highlight target selection
219 effects. Thus, in **Figure 4A**, we plotted activity contralateral and ipsilateral to the cue for each drug condition.
220 Cue direction modulated activity already early on, specifically from 70ms-336ms post-stimulus (two clusters:
221 70ms-125ms, p=.043, cluster-corrected; 141ms-336ms, p<.001; **Figure 4A/B**). The modulation of this activity
222 (averaged across both temporal clusters: 70-336ms) was similar for target and non-target stimuli (i.e.
223 contralateral/target vs. ipsilateral/non-target; $F_{1,27}$=0.06, p=.81, η_p^2=0.00, BF_{01}=3.44; not shown) and therefore
224 reflects an initial modulation of visual processing of any cued (attended) stimulus, irrespective of whether it was
225 a target or not. Moreover, effects of cue direction were not modulated by drug condition ($F_{2,54}$=0.11,
226 p=.99, η_p^2=0.00, BF_{01}=8.32; not shown)

After having established typical effects of spatial attention[43], we next tested whether drug condition modulated occipito-temporal activity. Indeed, drug condition affected ERP amplitudes, relatively late in time (406-586ms; p=.001 **Figure 4A**). Specifically, ATX showed a trend toward lower ERP amplitudes compared to PLC (t(27)=-1.89, p=.07, d=0.29; **Figure 4C**), whereas DNP increased amplitudes over occipito-temporal regions in this time-window (t(27)=2.21, p=.04, d=0.25). We did not observe any interaction effects between drugs and cue validity on activity in this time-window ($F_{2,54}$=0.37, p=.69, η_p^2=0.01, BF_{01}=6.43).

Next, we plotted activity split up for drug condition and hemisphere with relation to target location (i.e. contralateral and ipsilateral to target stimulus) in **Figure 4D**. We observed that contralateral activity (related to targets) was different from ipsilateral activity (related to non-targets) relatively late in time, from 352-500ms post-stimulus (p=.01; **Figure 4D/E**). As said, the difference between contralateral and ipsilateral activity in this window makes up the N2pc component. We show the N2pc in **Supplementary Figure S7**, which was not modulated by drug. Cue direction did not modulate the effect of target selection ($F_{1,27}$=0.01, p=.93, η_p^2=0.00, BF_{01}=4.07; not shown), showing that attentional and target selection processes occur at different latencies over occipital regions.

In sum, we observed three main effects and no interactions. Attentional effects modulated activity from early on (**Figure 4A**), whereas target selection and drugs modulations occur relatively late in time (**Figure 4A/C**). Although target selection and drug modulations overlap in time, there were no interactions.

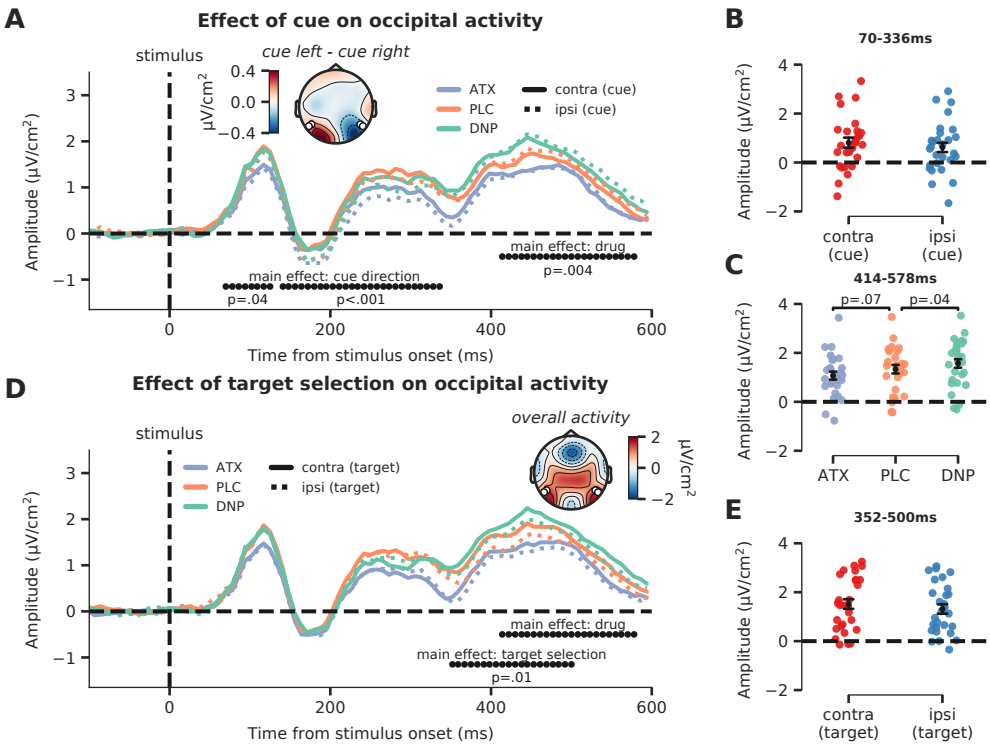

Figure 4. Modulation of perceptual processing by drug and attention, indexed by changes in occipito-temporal activity. A) Stimulus-locked ERPs (0ms = target presentation) over bilateral occipito-temporal ROIs (left hemifield: P7/P9 and right hemifield: P8/P10; see white markers in topographic map), showing activity over regions contralateral (solid) and ipsilateral (dashed) to the cue for each drug condition (averaged over cue validity). To isolate temporal clusters of interest we performed

3x2x2 (drug x cue validity x hemisphere) factor rmANOVAs across time (resolution of ~8ms) and controlled for multiple comparisons using cluster-based permutation testing [44]. Topographic map shows cue direction effect (contra – ipsi) across drug and attention conditions. Black dots indicate significant effects of rmANOVAs over time. **B)** Average activity within the first two temporal clusters from panel **A** related to cue direction. **C)** Activity within the late cluster of panel **C** for each of the three drug conditions. **D)** Same as panel **A**, but now split up for contralateral (solid) and ipsilateral (dashed) to the target stimulus (averaged over cue validity) and drug condition. Topographic map shows overall activity (no contrast) across drug and attention conditions. The drug cluster in this panel is identical to the cluster in panel **A**. **E)** Activity in late cluster of panel **D** related to target selection.

Neuromodulatory effects on preparatory attention

The predictive cues in our task allowed participants to anticipate targets appearing at certain locations, by covertly shifting their locus of attention. Previous work has identified a neural marker for attentional orienting in response to a visual cue, i.e. an early negative amplitude deflection over contralateral regions (early directing attention negativity, EDAN)[45,46]. Moreover, attentional shifts have been associated with changes in cortical excitability, indexed by lateralized alpha-band (8-12Hz) power suppression (stronger alpha suppression at the contralateral side of the stimulus)[47–50]. Recent studies also suggests that neuromodulatory systems may be involved in regulating changes in global cortical excitability in relation to shifts in spatial attention[29,51]. Here, we tested whether enhanced catecholaminergic and cholinergic levels modulated these electrophysiological markers of preparatory spatial attention. For the following EEG analyses, we used two symmetrical regions of interest (ROIs) over occipital areas that are commonly used for analyses regarding preparatory attention (left: O1, PO3 and PO7; right: O2, PO4 and PO8)[47,50,52].

First, we plotted the ERP locked to the onset of the attentional cue for contra- and ipsilateral ROIs, and for each drug condition, separately (**Figure 5A**). Neural activity in response to the cue was indeed strongly lateralized in two time-windows (89-175ms, p=.002; 198-363ms, p<.001). Interestingly, the early lateralized component (EDAN) was modulated by drug ($F_{2,54}$=5.05, p=.01, η_p^2=0.16; **Figure 5B**). This effect was driven by increased lateralization for ATX vs. PLC (t(27)=-4.89, p<.001, d=0.92; DNP vs. PLC: t(27)=-1.21, p=.24, d=0.23, BF_{01}=2.58). Lateralized activity in the later cluster was also modulated by drug ($F_{2,54}$=3.23, p=.047, η_p^2=0.11; **Supplementary Figure S8**), but pairwise post-hoc tests showed no reliable differences for ATX/DNP vs. PLC (ATX: t(27)=-1.20, p=.24, d=0.13, BF_{01}=2.60; DNP: t(27)=1.15, p=.26, d=0.13, BF_{01}=2.60).

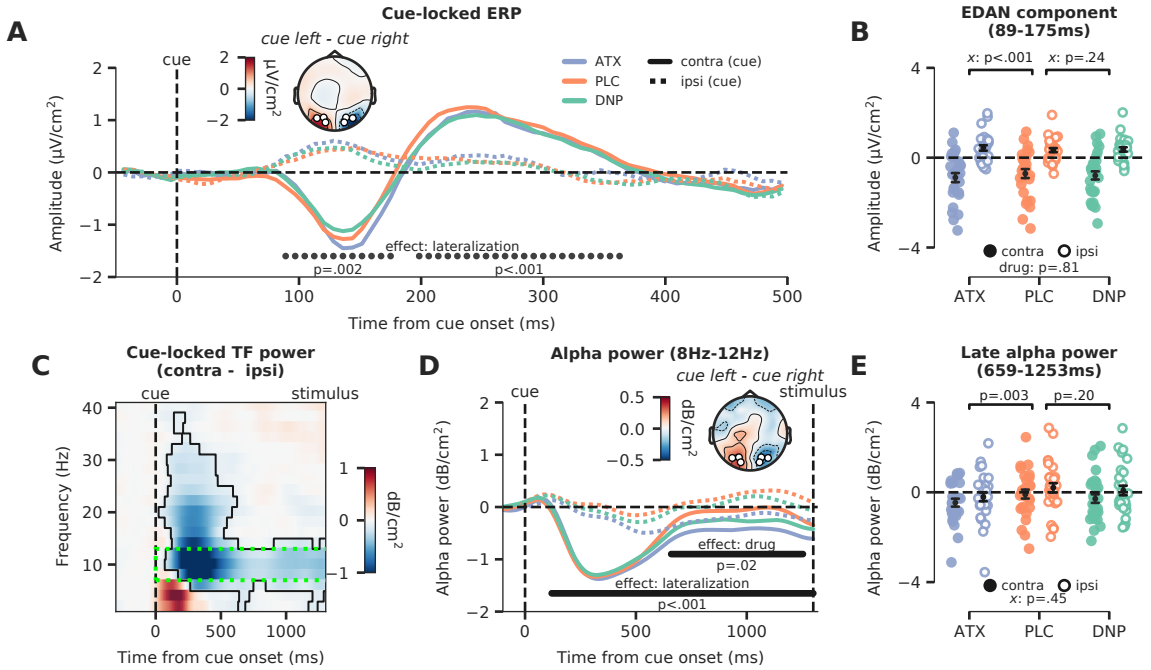

Figure 5. Attentional and catecholaminergic modulation of prestimulus cortical activity. A) Cue-locked ERP (µV/cm²) over occipital regions contralateral and ipsilateral to the predictive cue split up for three drug conditions. Black horizontal bars; rmANOVA main effects cluster corrected for multiple comparisons. Topographic map shows the contrast between cue directions (left vs. right) during the early lateralization cluster. White markers indicate spatial ROI used for analyses. **B)** Average activity within the early temporal cluster related to cue-locked hemispheric lateralization. **C)** Cue-locked modulations of lateralized (contra-ipsi) prestimulus time-frequency power (dB/cm²). The significant TF cluster (highlighted by the solid black line) is derived from cluster-based permutation testing controlling for multiple comparisons. Green dotted box indicates alpha-band time-frequency ROI that is used to compute panel **D**. **D)** Cue-locked prestimulus alpha power (dB/cm²) over occipital regions contralateral and ipsilateral to the predictive cue split up for three drug conditions. A cluster-base corrected 3x2 rmANOVA revealed that alpha power was modulated by hemisphere (lateralization effect) and drug. Topographic map shows the contrast between cue directions (left vs. right) during the cluster in which we observed a main effect of drug. **E)** Average alpha power within the late temporal cluster in which drug effects on alpha power were observed, split up for drug conditions and hemisphere.

Next, we focused on cue-locked alpha suppression dynamics from the onset of the attentional cue leading up to stimulus presentation (1300ms post-cue). Replicating previous work, the time-frequency (TF) spectrum plotted in **Figure 5C** shows that attentional cues resulted in a stronger suppression of alpha power over contralateral (to location of spatial cue) compared to ipsilateral channels. To test the effects of drug and lateralization, and their potential interaction, on prestimulus excitability, we plotted alpha power (8-12 Hz) for contra- and ipsilateral channels for all 3 drug conditions separately in **Figure 5D**. Significant alpha lateralization was observed 120ms from cue onset until target stimulus onset (p<.001; **Figure 5D**). Moreover, total alpha power, across both hemispheres, was modulated by drug from 659-1253ms after cue onset (p=.02; **Figure 5D**). Again, this main effect of drug was driven by catecholaminergic activity (ATX vs. PLC t(27)=-3.23, p=.003, d=0.38; DNP vs PLC t(27)=-1.32, p=.20, d=0.15, BF_{01}=2.29; **Figure 5E**).

301 When we binned trials according to the level of alpha suppression in the late time window, we observed a
302 significant interaction between cue validity and alpha power lateralization on d' ($F_{1,27}$=5.14, p=.03, η_p^2=0.16;
303 **Supplementary Figure S9**). This shows that efficient allocation of attention aids performance for validly cued
304 trials but harms performance when the target is presented at the unattended location. Enhanced
305 neuromodulatory activity did not alter this relationship (3-way interaction: $F_{2,54}$=0.63, p=.54, η_p^2=0.02, BF_{01}=4.33;
306 **Supplementary Figure S9**).

307 Thus, ATX increased cue lateralization effects suggesting enhanced attentional orientation **(Figure 5A).** However,
308 prestimulus occipital alpha power (an index of cortical excitability[47–50]) was bilaterally decreased under ATX
309 suggesting instead that enhanced catecholaminergic levels regulate cortical excitability in a spatially non-specific
310 manner (**Figure 5C**). Contrarily, cue direction was associated with a relative suppression of alpha power over
311 contralateral regions. We did not observe any interaction effects between cue direction and drug condition as
312 well, showing that spatial attention and tonic neuromodulation differentially control cortical excitability.

313 Discussion

314 Fluctuations in arousal state and selective attention have a profound impact on perceptual processing and
315 decision making. Both attention and arousal state, the latter under the influence of global neuromodulation,
316 determine the input-output ratio of neurons and neural networks, consequently modulating the responsiveness
317 to internal and external signals[10,14,21,53]. Here, we used a 3x2 factorial design in which we manipulated spatial
318 attention and neuromodulator levels, allowing us to investigate their separate and shared effects on perceptual
319 decision-making by examining the processes leading up to a categorical decision about a visual stimulus. By
320 administering atomoxetine (ATX) and donepezil (PLC) to healthy human participants, we were able to tease apart
321 the roles of cholinergic and catecholaminergic neuromodulatory systems respectively, in relation to, and in
322 interaction with, spatial attention. We show that increased catecholaminergic activity and allocation of attention
323 to target stimuli both improve perceptual sensitivity (**Figure 2A**, see also[54]). Subsequent drift diffusion modeling
324 showed that both factors did so by enhancing the rate of sensory evidence accumulation (**Figure 2D**). Moreover,
325 effects of attention on drift rate were enhanced under catecholaminergic enhancement.

326 Although the effects of attention and catecholaminergic neuromodulation on perceptual decision-making were
327 very similar at the behavioral level, our EEG analyses point towards different sources of these behavioral effects.
328 First, although both attention and catecholaminergic enhancement affected centro-parietal decision signals in
329 the EEG related to evidence accumulation[40,41], attention mainly affected the build-up rate (slope) whereas ATX
330 increased the amplitude of the CPP component (**Figure 3D-F**). Note that although both CPP peak amplitude and
331 build-up rate modulations have been observed before, it is not yet clear how to interpret the roles of these
332 component features in an accumulation-to-threshold framework[55]. Second, increases in sensory evidence
333 accumulation, reflected in the CPP, were preceded by attentional and catecholaminergic modulations of activity
334 over occipito-temporal electrodes earlier in time. However, attention modulated cortical processing much earlier
335 in time (starting ~70ms after stimulus presentation) than the catecholaminergic intervention (starting ~350ms
336 after stimulus presentation; **Figure 4A**, **Supplementary Figure S7**). Third, both spatial attention and

catecholamines modulated cortical excitability, as reflected in in alpha-band desynchronization (**Figure 5D**), but attention did so unilaterally (opposite to the locus of attention) and catecholamines did so bilaterally (no hemispherical specificity nor interaction with attentional lateralization effect). These findings are in line with recent work showing independent modulations of spatial attention and arousal on neuronal activity in mouse V1[56]. In conclusion, although the effects of spatial attention and global catecholaminergic activity were ostensibly similar in terms of behavior, they were separable in terms of CPP component feature (amplitude vs slope), latency of evoked sensory processes (early vs late), and spatial specificity (hemisphere specific vs. global) showing that spatial attention and tonic neuromodulator levels differentially contribute to processing of sensory input.

So far, previous work has mainly used correlational methods to explore how neuromodulation levels affect perceptual and decision-making processes in humans (for exception see e.g.[54]). These studies have often linked performance on simple discrimination or detection tasks to different readouts of fluctuations in brain state, most prominently spontaneous variations in pupil size[26,57–59], alpha-band power modulations[7,8,60–64], or both simultaneously[58,65]. Pupil diameter is thought to reflect an indirect and continuous readout of arousal state, ranging from aroused (wide pupils) to unaroused (constricted pupils) levels[66,67]. Although several animal studies have observed a tight link between pupil size, locomotor activity (running vs quiescence) and cortical variability and/or neural desynchronization, at present it is unclear how these measures of global brain state are related, whether they are signatures of the same underlying mechanism and whether similar mechanisms influence human perception as well. Moreover, recent work suggests that pupil diameter may in fact be a less accurate readout of Locus Coereleus (i.e. the nucleus involved in synthesis of noradrenaline) activity than previously thought, and as such may not be optimal to establish relations between arousal levels and perception[68]. By pharmacologically manipulating arousal, we were able to demonstrate a causal relationship between neuromodulator activity and visual perception in human subjects.

As predicted, this work shows that the effects of neuromodulator activity are relatively global and non-specific, whereas the effects of spatial attention are more specific to certain locations in space. This is, however, in contrast with recent work associating catecholaminergic and cholinergic activity with attention by virtue of modulating prestimulus alpha-power shifts[30,51] and cue-locked gamma-power[29,69]. However, our findings are not necessarily at odds with these studies. Most importantly, in our work we specifically investigated the effects of tonic (baseline) levels of neuromodulation by suppressing reuptake or breakdown of catecholamines and acetylcholine throughout cortex and subcortical structures. Contrarily, most recent work associates phasic (event-related) arousal with selective attention[21,51]. For example, cue detection in visual tasks is known to be related to cholinergic transients occurring after cue onset[69,70]. Because phasic and tonic activity are thought to be anti-correlated, with lower phasic responses following high baseline activity and vice versa[59,71], pharmacologically increasing tonic arousal may have resulted in relatively weaker phasic activity. This in turn could have resulted in sub-optimal cue processing. This would be in line with electrophysiological recordings in rat medial prefrontal cortex, showing that detected cues are preceded by waning cholinergic activity and followed by strong phasic responses – and vice versa[70]. Moreover, although we mostly observed separable effects of spatial attention and arousal on neural signals, the effects of attention on behavioral drift rate were

enhanced under catecholaminergic enhancement (**Figure 2D**). Since this interaction effect was not observed in neural markers of target selection and evidence accumulation, the neural basis for enhanced attentional effects on drift rate under higher levels of arousal remains elusive.

So far, it has remained unclear whether fluctuations in arousal states actually affect the sensory build-up of perceptual representations or whether they mostly affect response criterion or other latent variables of the decision process[9]. For example, human work on alpha-band dynamics and perception has not yet been able to arbitrate between the hypothesis that decreased alpha-band power may reflect an overall increase in baseline excitability (resulting in amplified responses to both signal and noise) or whether baseline excitability may decrease/increase the trial-by-trial precision of neural responses. The first case would result in alterations in response criterion, whereas the latter case would lead to less/more accurate perceptual performance and improved sensitivity[6,9,61,63,64,72]. The same issue is crucial in studying the influence of other contextual factors on perception/behavior, such as serial dependencies of stimuli or choices[37,73,74]. Here we provide evidence that the effects of arousal seem to manifest relatively late in time, close to the decision stage[24–26,54,75], whereas the effects of attention were observable at relatively early stages in the cortical hierarchy, in line with a large body of work[76–79]. Our findings do not settle the debate on the role of prestimulus excitability on perceptual decision making, but do highlight that cortical excitability is under the control of various factors -such as attention and arousal- that shape sensory processing differentially and therefore need to be considered when addressing the effect of prestimulus excitability on perception.

We did not observe consistent subjective, physiological or behavioral effects of DNP, although the dosage of 5mg was identical to previous studies using DNP as a cholinergic stimulant[33–36,80]. Note that the only non-clinical studies that report physiological responses of DNP (most studies do not report these effects), show no bodily arousal effects either[33,34]. However, even in the absence of such autonomic markers, 5mg DNP has been shown to induce behavioral and neural effects, related to visual perception[33–36,80]. Although DNP did not significantly affect perceptual sensitivity and/or drift rate, we did observe a set of consistent neural effects, generally reflected in neural responses in the opposite direction as for ATX. This was the case for the CPP peak and slope (**Figure 3D-F**) as well as for occipito-temporal signals related to target selection and cue processing (**Figure 4A/C**, **Figure 5A-B**). This is in line with a similar observation in an auditory oddball task, where nicotine (a cholinergic agonist of the nicotine receptor) decreased the amplitude of the P3b, an ERP component often linked to the CPP, but only for individuals with strong baseline P3b responses (this effect may have been driven by regression to the mean, also acknowledged by the authors)[81]. One reason why DNP may show opposite effects compared to ATX is that high ACh levels are associated with enhanced magnitudes of afferent input to cortex (feedforward) but decreased excitatory feedback[15]. Evidence accumulation processes and target selection processes strongly rely on cortical feedback[82–91] and therefore the mirrored effects of DNP compared to ATX may have been caused by interrupted feedback processing. This interpretation is supported by a recent study using DNP and ATX in combination with whole-brain fMRI, which revealed that these neuromodulator systems have opposite effects on cortex-wide connectivity patterns, even though both systems enhanced neural gain[34]. More specifically, catecholamines enhanced and acetylcholine suppressed cortex-wide auto-correlation of activity[34], suggested to

411 reflect reduced intracortical signaling by lateral and feedback processes[15,80]. Future work applying various
412 stimulants and suppressors of cholinergic activity is necessary to further unravel the relationship between
413 cholinergic neuromodulation and spatial attention as well. Although previous work has implicated the cholinergic
414 system in pre-stimulus alterations in neural excitability, indexed by alpha-power desynchronization, we did not
415 find evidence for this (**Figure 5E**), possibly because this study used physostigmine, a more potent cholinergic
416 esterase inhibitor than DNP[92]. Future work using different cholinergic stimulants, administered in different doses,
417 is necessary to firmly establish the role of the cholinergic system in controlling cortical excitability and spatial
418 attention.

419 Summarizing, we show that tonic arousal and spatial attention jointly shape visual perception and consequent
420 decision-making, by modulating the rate at which sensory evidence is accumulated over time. Although
421 behavioral effects of tonic global arousal and spatial attention were seemingly identical, neural measures
422 indicated that their respective effects differed with regard to spatial specificity, timing and ERP component
423 feature. These findings highlight how arousal state and selective attention strongly influence processing and
424 interpretation of sensory input and as such are key components in perception.

425

426 # Methods

427 ## Participants

428 For this experiment 30 male, Dutch-speaking, human participants were recruited from the online research
429 environment of the University of Amsterdam. All participants were aged between 18 and 30. Given the
430 pharmacological nature of this experiment, participants were only included after passing extensive physical and
431 mental screening (see **Screening procedure**). This study was approved by the Medical Ethical Committee of the
432 Amsterdam Medical Centre (AMC) and the local ethics committee of the University of Amsterdam. Written
433 informed consent was obtained from all participants after explanation of the experimental protocol. Two
434 participants decided to withdraw from the experiment after having performed the first experimental session.
435 The data from these participants are not included in this work, resulting in N=28.

436 ## Screening procedure

437 Following registration, candidate participants were contacted via e-mail to inform them of the inclusion criteria,
438 exact procedures, and possible risks. In addition, candidate participants were provided with the credentials of an
439 independent physician that was available for questions and further explanation. The participants were contacted
440 after a deliberation period of seven days to invite them for a pre-intake via telephone. During this pre-intake, it
441 was ensured that the candidate participant indeed met all inclusion and exclusion criteria (for a complete list of
442 criteria see **Supplementary Information**). If so, participants were invited for an intake session at the research
443 facility of the University of Amsterdam. During this in-person intake, the experimental protocol, including the
444 following physical and mental assessment, was explained in detail after which candidate participants provided
445 written consent. The intake further consisted of a set of physiological measures -body mass index (BMI), heart-

446 rate, blood pressure, and an electrocardiogram (ECG)- and a psychiatric questionnaire to assess mental health.
447 The data from the intake were assessed by a physician, who subsequently decided whether a candidate
448 participant was eligible for participation. Lastly, participants performed the staircasing procedure for the
449 behavioral task (see **Staircasing procedure**).

450 **Drug administration**

451 The study was conducted using a randomized, double-blind crossover design. Atomoxetine (40mg), donepezil
452 (5mg) and placebo were administered in different experimental sessions, separated by at least seven days. The
453 order of drug administration was counterbalanced between participants. Experimental days started at 09:00 and
454 ended at 16:00. Atomoxetine (~2 hours) and donepezil (~4 hours) reach peak plasma levels at different latencies,
455 therefore these pharmaceuticals were administered at different times prior to the onset of the behavioral tasks
456 (**Figure 1A**). To ensure the double-blind design, participants were required to orally ingest a pill 4 hours prior to
457 the onset of the first behavioral task, which could contain either donepezil or a placebo, and a second pill 2 hours
458 prior to onset of the first behavioral task, which could contain either atomoxetine or a placebo. Thus, participants
459 received one placebo and a working pharmaceutical or two placebos on every experimental session. For more
460 information on atomoxetine and donepezil see the **Supplementary Information**.

461 **Design and procedures**

462 Experimental setting

463 Participants performed several tasks during a single experimental day. The first task was an auditory
464 discrimination/detection task, lasting two hours, that was executed directly after the administration of the first
465 pill. The data of that experiment fall outside the scope of this paper. An EEG apparatus was connected 3.5 hours
466 after ingestion of the first pill, ensuring that participants could start the main experiment precisely 4 hours after
467 ingestion of the first pill, supposedly when blood concentration levels for both atomoxetine and donepezil were
468 peaking. During this main part of the experiment participants performed five different computerized visual
469 perception tasks, out of which we will only discuss the spatial attention task. The order of these behavioral tasks
470 was counterbalanced between participants but was maintained over sessions. Participants were seated in a
471 darkened, sound isolated room, resting their chins on a head-mount located 80cm from a 69x39cm screen
472 (frequency: 60Hz, resolution: 1920 x 1080). The main task and staircase procedure were programmed in Python
473 2.7 using PsychoPy[93] and in-house scripts.

474 Cued orientation discrimination paradigm

475 Participants performed a task that was adapted from the Posner cueing paradigm[94]. For the task, participants
476 were asked to report the orientation of Gabor patches as being clockwise (45°) or counterclockwise (-45°), by
477 pressing left ("s" on a keyboard, for counterclockwise) or right ("k", for clockwise) with their left or right index
478 finger respectively. We did not specifically instruct participants to respond as quickly or accurately as possible.
479 The Gabor patches were presented for 200ms on either the left or right side of the screen (center at 8°, radius
480 5.5°, spatial frequency 1.365 cycles/degree). Simultaneously, circular patches containing dynamic noise were
481 presented bilaterally (center at 8°, radius 6.5°). Prior to stimulus presentation, a visual cue was presented for

300ms near the fixation mark (horizontal dash, center at 0.33°). This cue was predictive of the stimulus location with a cue validity of 80%, meaning that the cue matched the stimulus location in 80% of the trials. Participants were instructed to use the cue, by covertly shifting attention (i.e. without moving eyes) towards the cued location. In 20% of trials the cue was invalid and the stimulus would appear on the opposite side. After cue offset there was a 1000ms interval until stimulus onset. The response window started concurrently with stimulus presentation and lasted 1400ms. If participants did not respond during this window they would receive visual feedback informing them of their slow response (in Dutch: "te laat", which translates into: "too late"). A variable inter-trial interval (ITI) of (250ms-350ms) started directly after a response or the end of the response-window. Stimulus locations, stimulus orientation and cue direction were all balanced to occur on 50% of the trials (i.e. 50% counterclockwise, 50% left location, 50% cue to the right etc.). The task was divided in two blocks of 280 trials, which in turn were subdivided in shorter blocks of 70 trials, in between which the participants could rest.

To ensure participants did not shift their gaze towards either the left or right, we measured gaze position via eyetracking (see **eyetracking**). Trials only commenced when participants' gaze was at fixation (cutoff: 1.5°) and whenever participants lost fixation or blinked during a trial, the fixation mark would turn white and the data for the trial would be marked as faulty. At the end of each block, a new trial was presented for every trial that was terminated because of blinks or lost fixation. In total, participants performed 560 trials of this task without losing fixation or blinking. After 280 trials on which fixation was not lost, the eyetracker was recalibrated (see **Eyetracking)**.

Staircasing procedure

Participants performed a staircasing procedure during their intake session. The staircase task was almost identical to the primary task, but without predictive cues prior to stimulus onset. The stimulus properties, presentation time and response window were the same. The ITI was prolonged to 1100ms-1300ms. Participants received feedback on their performance on a trial-by-trial basis; the fixation dot turned green for correct answers and red for incorrect answers. An adaptation of the weighted up-down method proposed by Kaernbach (1991) was used to staircase performance at 75% correct, by changing the opacity of the Gabor patch. In short, opacity adjustment after erroneous responses were weighted differently than after correct responses, in a ratio of 3:1. The step size was 0.01 (opacity scale: 0-1, 1 is fully opaque), thus after errors the opacity would be increased by 0.01 and after correct answers it would be decreased by 0.01/3. The procedure was aborted after 50 behavioral reversals, i.e. changes in sequences from correct to error or vice versa. The output difficulty of the staircase procedure was calculated as the average opacity on reversal trials. In total, participants performed two blocks of this staircase procedure. The first block started at a high opacity, allowing the participants to become familiar with the stimulus. The second block started at the opacity obtained from the first block. After completing the staircasing procedure, task difficulty was fixed to be able to compare the effects of the pharmacological manipulation across all experimental sessions.

Data acquisition and preprocessing

Eyetracking

Gaze position and pupil size were measured with an EyeLink 1000 (SR Research, Canada) eyetracker during the experiment at 1000Hz. Gaze position was moreover monitored online to ensure participants' gaze remained at or near fixation (within 1.5°, horizontal axis). A nine-point calibration was used at the start of each block. To minimize movement of the participant, we used a head-mount with chinrest. Throughout the experiment participants were instructed to move their heads as little as possible and to try to refrain from blinking during a trial. Pupil traces were bandpass filtered between 0.01Hz-10Hz, blinks were linearly interpolated and the effects of blinks and saccades on pupil diameter were removed via finite impulse-response deconvolution[71].

<u>EEG acquisition, preprocessing and time-frequency decomposition</u>

EEG-data were recorded with a 64-channel BioSemi apparatus (BioSemi B.V., Amsterdam, The Netherlands), at 512Hz. Vertical eye-movements were recorded with electrodes located above and below the left eye, horizontal eye-movements were recorded with electrodes located at the outer canthi of the left and the right eye. All EEG traces were re-referenced to the average of two electrodes located on the left and right earlobes. The data were high-pass filtered offline, with a cut-off frequency of 0.01Hz. Next, bad channels were detected automatically via a random sample consensus algorithm (RANSAC), implemented in the Autoreject Python package[96], and subsequently interpolated via spline interpolation. Next, epochs were created by taking data from -2000ms to 2000ms around onset of stimulus presentation. To remove eyeblink artefacts, an independent component analysis (ICA; 25 components) was performed on the epoched data and components that strongly correlated to vertical EOG data were excluded. On average 1.23 (sd: 0.47, maximum: 3) components were rejected per file. Remaining artefacts were automatically detected by using the same RANSAC algorithm as before but on epoched data. Bad segments were repaired via interpolation if the artifactual data was present in only a few channels, but if more channels were affected the epoch was removed from the EEG data. On average 3.82% (sd: 5.16, maximum: 24.18%) of all epochs were removed. Lastly, the scalp current density was computed using the surface Laplacian to attenuate the effects of volume conductance[97].

Time-frequency (TF) representations of EEG data were calculated from epochs that were extracted from a time-window -1600ms to 0ms pre-stimulus. Time-frequency power was obtained through convolution of Morlet wavelets with epoched data from 2-40Hz in steps of 2Hz. For each frequency, we defined the amount of cycles as:

I. $\text{number cycles (f)} = \frac{\text{f}}{2}$

Then we averaged TF data across cue validity conditions and spatial locations (four stimulus categories). Next, both this average TF power, as well as single trial TF power, was normalized to a baseline of -250ms to -50ms pre-cue with a decibel (dB) transformation:

II. $\text{Power (dB)} = 10 * \log_{10} \frac{\text{signal}}{\text{baseline}}$

Data analysis

All behavioral analyses were programmed in Python 3.7. Trials during which fixation was lost missed trials and trials with a reaction time (RT) larger than 1400ms were excluded from all analyses. The remaining data was used

553 for the main behavioral analyses, but for the alpha power binning analysis of **Supplementary Figure S9,** only
554 behavioral data belonging to unrejected EEG epochs were included in order to match single trial EEG to behavior.
555 EEG analyses were performed with use of the Python package MNE (version 0.24.0)[98].

556 Statistical analysis of physiological data, side-effects and self-reports

557 We obtained bodily (heart rate and blood pressure) and subjective (Visual Analogue Scale, VAS[99]) measurements
558 of arousal on three occasions during each session; before drug intake (baseline), prior to the onset of the first
559 EEG task (t=4 hours) and at the end of each session (t=7hours). We calculated mean arterial pressure (MAP) from
560 systolic and diastolic blood pressure as:

561 III. $$\text{mean arterial pressure} = \text{diastolic BP} + \frac{1}{3} * (\text{systolic BP} - \text{diastolic BP})$$

562 VAS scores were calculated by measuring the location of marked answers in centimeters from the left. Next, all
563 16 scores of the VAS were into three categories: contentedness, calmness and alertness following previous
564 methods[100]. HR, MAP and VAS scores were corrected by calculating percentage change from the baseline
565 measurement. Next, we applied 1-factor rmANOVAs (factor drug), on these scores for each of the remaining
566 timepoints. Post-hoc, pairwise t-tests were performed to test the effects of ATX and DNP vs. PLC.

567 We asserted the effects of drug on pupil diameter right before the onset of the behavioral tasks (at t=4 hours).
568 We defined minimal (bright monitor background) and maximal (dark monitor background) pupil diameter as the
569 average pupil size within the final 5s of each presentation window of 15s. Next, we performed similar rmANOVAs
570 and post-hoc t-tests on these raw (non-normalized) pupil diameters. To test the occurrence of side effects as
571 well proportion of forced guesses of drug intake at the end of each session, we used binomial tests. Specifically,
572 we calculated proportions of side-effects and guesses about the nature of drug intake (placebo or
573 pharmaceutical) under PLC. Then we calculated the same proportions for ATX and DNP and tested them against
574 the PLC proportion with a binomial test.

575 Statistical analysis of behavioral data

576 To investigate behavioral performance on this task, we used perceptual sensitivity (d') and bias (criterion) derived
577 from signal detection theory (SDT)[22] in addition to RTs. To test the effect of cue validity and drugs on these
578 measures we performed 3x2 factorial rmANOVAs (factors: drug and cue validity). We did not include drug order
579 as a between-subject variable in our statistical models, because drug order was counter-balanced between
580 participants. Bayesian rmANOVAs (uniform prior, default setting) and t-tests (Cauchy scale=0.707, default
581 setting) were used in the case of null-findings, to test support for the null-hypothesis[101].

582 Drift diffusion modelling

583 We constructed a drift diffusion model (DDM) to gain insight into which parameters of the decision process were
584 modulated by attention and tonic arousal[23]. Specifically, we used the Python package HDDM to fit hierarchical
585 Bayesian accuracy-coded regression models to reaction time distributions of correct and incorrect trials for every
586 subject[102]. In a first regression model, we allowed drift rate, non-decision time and decision bound separation to
587 vary with drug, cue validity and their interaction. To estimate the effects of drug, we fitted these regression

588 models separately for ATX (versus placebo) and DNP (versus placebo). We applied a weighted effect coding
589 scheme, meaning that we coded our regressors as -1 and 1 (instead of dummy coding: 0 and 1). We weighted
590 the regressors for cue validity according to the proportion of valid and invalid trials (-0.8 for invalid, 0.2 for valid),
591 because valid and invalid trial counts were unbalanced. The effects of this model can be interpreted similarly as
592 effects derived from an ANOVA. The Bayesian implementation of this model constrained single subject
593 parameter estimates on the basis of population estimates, making the model more robust to noise. Note that
594 we also fitted unweighted effect coded versions of these models to verify the output of our weighted models, as
595 well as two additional (weighted effect-coded) models to test whether drift rate variability was also modulated
596 by cue validity and arousal (**Supplementary Information**)[39].

597 EEG - ERP analysis

598 To assert how spatial attention and tonic arousal shape visual perception, we looked at neural activity related to
599 the processing of the visual input (cue and stimulus) as well as activity related to the sensory information
600 accumulation process preceding the response. For statistical analyses, epoched data were downsampled to
601 128Hz. We used distinct spatial ROIs for each of these events, based on previous literature. For cue processing,
602 we used symmetrical electrode pairs O1/O2, PO3/PO4, and PO7/PO8[47,50,52], for processing of the visual stimulus,
603 we used the symmetrical electrode pairs P7/P8 and P9/P10 and for response-locked evidence accumulation
604 signals (i.e. centroparietal positivity, CPP) we used electrodes CPz, Cp1, and Cp2[26,38,40]. To calculate these ERPs,
605 we first normalized epochs by subtracting the average baseline activity -80ms to 0ms before cue onset (for cue-
606 locked ERP) and stimulus onset (for stimulus-locked and response-locked ERP).

607 We calculated the peak amplitude of the CPP as the amplitude at the time of the response and the slope of the
608 CPP by fitting a linear regression in a time-window ranging from -250ms to 0ms before the response. Note that
609 the time-window used for CPP slope estimation was chosen on the basis of visual inspection of the grand average
610 CPP and roughly coincided with previous time-windows used for slope estimation[26,38]. Next, CPP peak amplitude
611 and slope were tested for incorrect vs. correct and fast vs. slow response trials (median split) with two-sided
612 pairwise t-tests and for high vs. low drift rate participants with independent t-tests (**Figure 3A-C**). Moreover, 2x3
613 (attention x drug) rmANOVAs and post-hoc two-sided t-tests (drug vs. placebo) were used to test the effects of
614 cue validity and drug on CPP slope and peak amplitude. We further used cluster-corrected rmANOVAs over time
615 to establish the effects of target vs. non-target information, spatial attention, cue validity and drug on cue-locked
616 and stimulus-locked ERP data. Lastly, we extracted activity from significant clusters, to test for other main and
617 interaction effects.

618 We analyzed stimulus-locked ERPs with a cluster-corrected permutation (5000 permutations) 3x2x2 (drug x
619 hemisphere x cue/stimulus location) rmANOVA. Note that in **Figure 4**, the same data was statistically analyzed
620 and plotted, although the labels were rearranged to be able to plot activity contralateral and ipsilateral to the
621 cue in **Figure 4A** and activity contralateral and ipsilateral to the target stimulus in **Figure 4D**. For the cue-locked
622 ERP (**Figure 5A**), we performed a cluster-corrected permutation (5000 permutations) 3x2 (drug x hemisphere)
623 rmANOVA.

624 EEG - time-frequency analysis

625 To test the effects of spatial attention and tonic arousal on cortical excitability, we calculated the lateralization
626 of TF power (contralateral – ipsilateral) across cue validity and drug conditions and then tested this lateralization
627 against zero with cluster-corrected two-sided permutation tests (5000 permutations; **Figure 5C**). Furthermore
628 we extracted power from the alpha-band (8-12Hz) and tested the effects of hemisphere (contralateral vs.
629 ipsilateral to cue) and drug condition on power within this frequency band with a cluster-corrected permutation
630 (5000 permutations) 3x2 (drug x hemisphere) rmANOVA. Lastly, we extracted lateralized single trial alpha power
631 from the late cluster plotted in **Figure 5D** and binned data according to prestimulus alpha power in two evenly
632 sized bins. Then, for every bin and cue validity condition we calculated d' and tested the effects of drug,
633 prestimulus alpha power bin and cue validity on d' with a 3x2x2 rmANOVA (**Supplementary Figure S9**).

References

1. Gold, J. I. & Shadlen, M. N. The Neural Basis of Decision Making. *Annu. Rev. Neurosci.* **30**, 535–574 (2007).
2. Renart, A. & Machens, C. K. Variability in neural activity and behavior. *Curr. Opin. Neurobiol.* **25**, 211–220 (2014).
3. Wyart, V. & Koechlin, E. Choice variability and suboptimality in uncertain environments. *Curr. Opin. Behav. Sci.* **11**, 109–115 (2016).
4. Waschke, L., Kloosterman, N. A., Obleser, J. & Garrett, D. D. Behavior needs neural variability. *Neuron* **109**, 751–766 (2021).
5. Benwell, C. S. Y., Tagliabue, C. F., Veniero, D., Cecere, R., Savazzi, S. & Thut, G. Prestimulus EEG Power Predicts Conscious Awareness But Not Objective Visual Performance. *eneuro* **4**, ENEURO.0182-17.2017 (2017).
6. Busch, N. A., Dubois, J. & VanRullen, R. The Phase of Ongoing EEG Oscillations Predicts Visual Perception. *J. Neurosci.* **29**, 7869–7876 (2009).
7. Iemi, L., Chaumon, M., Crouzet, S. M. & Busch, N. A. Spontaneous neural oscillations bias perception by modulating baseline excitability. *J. Neurosci.* **37**, 807–819 (2017).
8. Iemi, L., Gwilliams, L., Samaha, J., Auksztulewicz, R., Cycowicz, Y. M., King, J.-R., Nikulin, V. V., Thesen, T., Doyle, W., Devinsky, O., Schroeder, C. E., Melloni, L. & Haegens, S. Ongoing neural oscillations influence behavior and sensory representations by suppressing neuronal excitability. *NeuroImage* **247**, 118746 (2022).
9. Samaha, J., Iemi, L., Haegens, S. & Busch, N. A. Spontaneous Brain Oscillations and Perceptual Decision-Making. *Trends Cogn. Sci.* **24**, 639–653 (2020).
10. Harris, K. D. & Thiele, A. Cortical state and attention. *Nat. Rev. Neurosci.* **12**, 509–523 (2011).
11. Summerfield, C. & Egner, T. Expectation (and attention) in visual cognition. *Trends Cogn. Sci.* **13**, 403–409 (2009).
12. Carrasco, M. Visual attention: The past 25 years. *Vision Res.* **51**, 1484–1525 (2011).
13. Desimone, R. & Duncan, J. Neural mechanisms of selective visual attention. *Annu. Rev. Neurosci.* **18**, 193–222 (1995).
14. Aston-Jones, G. & Cohen, J. D. An Integrative Theory of Locus Coereleus-Norepinephrine function: Adaptive Gain and Optimal Performance. *Annu. Rev. Neurosci.* **28**, (2005).
15. Hasselmo, M. E. & Sarter, M. Modes and Models of Forebrain Cholinergic Neuromodulation of Cognition. *Neuropsychopharmacology* **36**, 52–73 (2011).
16. McCormick, D. A. Cholinergic and noradrenergic modulation of thalamocortical processing. *Trends Neurosci.* **12**, 215–221 (1989).
17. McGinley, M. J., David, S. V. & McCormick, D. A. Cortical Membrane Potential Signature of Optimal States for Sensory Signal Detection. *Neuron* **87**, 179–192 (2015).
18. Hillyard, S. A., Vogel, E. K. & Luck, S. J. Sensory gain control (amplification) as a mechanism of selective attention: electrophysiological and neuroimaging evidence. *Philos. Trans. R. Soc. B Biol. Sci.* **353**, 1257–1270 (1998).
19. Soma, S., Shimegi, S., Osaki, H. & Sato, H. Cholinergic modulation of response gain in the primary visual cortex of the macaque. *J. Neurophysiol.* **107**, 283–291 (2012).
20. Martinez-Trujillo, J. C. & Treue, S. Feature-Based Attention Increases the Selectivity of Population Responses in Primate Visual Cortex. *Curr. Biol.* **14**, 744–751 (2004).

21. Thiele, A. & Bellgrove, M. A. Neuromodulation of Attention. *Neuron* **97**, 769–785 (2018).

22. Green, D. M. & Swets, J. A. *Signal detection theory and psychophysics*. xi, 455 (John Wiley, 1966).

23. Ratcliff, R. & McKoon, G. The Diffusion Decision Model: Theory and Data for Two-Choice Decision Tasks. *Neural Comput.* **20**, 873–922 (2008).

24. Loughnane, G. M., Brosnan, M. B., Barnes, J. J. M., Dean, A., Nandam, L. S., O'Connell, R. G. & Bellgrove, M. A. *Catecholamine modulation of evidence accumulation during perceptual decision formation; a randomised trial*. http://biorxiv.org/lookup/doi/10.1101/470120 (2018) doi:10.1101/470120.

25. Nieuwenhuis, S., Aston-Jones, G. & Cohen, J. D. Decision making, the P3, and the locus coeruleus--norepinephrine system. *Psychol. Bull.* **131**, 510–532 (2005).

26. van Kempen, J., Loughnane, G. M., Newman, D. P., Kelly, S. P., Thiele, A., O'Connell, R. G. & Bellgrove, M. A. Behavioural and neural signatures of perceptual decision-making are modulated by pupil-linked arousal. *eLife* **8**, e42541 (2019).

27. Eimer, M. The N2pc component as an indicator of attentional selectivity. *Electroencephalogr. Clin. Neurophysiol.* 225–234 (1996).

28. Loughnane, G. M., Newman, D. P., Bellgrove, M. A., Lalor, E. C., Kelly, S. P. & O'Connell, R. G. Target Selection Signals Influence Perceptual Decisions by Modulating the Onset and Rate of Evidence Accumulation. *Curr. Biol.* **26**, 496–502 (2016).

29. Bauer, M., Kluge, C., Bach, D., Bradbury, D., Heinze, H. J., Dolan, R. J. & Driver, J. Cholinergic Enhancement of Visual Attention and Neural Oscillations in the Human Brain. *Curr. Biol.* **22**, 397–402 (2012).

30. Dahl, M. J., Mather, M., Sander, M. C. & Werkle-Bergner, M. Noradrenergic Responsiveness Supports Selective Attention across the Adult Lifespan. *J. Neurosci.* **40**, 4372–4390 (2020).

31. Simpson, D. & Plosker, G. L. Atomoxetine: a review of its use in adults with attention deficit hyperactivity disorder. *Drugs* **64**, 205–222 (2004).

32. Rogers, S. L. & Friedhoff, L. T. Pharmacokinetic and pharmacodynamic profile of donepezil HCl following single oral doses. *Br. J. Clin. Pharmacol.* **46**, 1–6 (1998).

33. Pfeffer, T., Avramiea, A.-E., Nolte, G., Engel, A. K., Linkenkaer-Hansen, K. & Donner, T. H. Catecholamines alter the intrinsic variability of cortical population activity and perception. *PLOS Biol.* **16**, e2003453 (2018).

34. Pfeffer, T., Ponce-Alvarez, A., Tsetsos, K., Meindertsma, T., Gahnström, C. J., Brink, R. L. van den, Nolte, G., Engel, A. K., Deco, G. & Donner, T. H. Circuit mechanisms for the chemical modulation of cortex-wide network interactions and behavioral variability. *Sci. Adv.* **7**, eabf5620 (2021).

35. Boucart, M., Bubbico, G., szaffarczyk, S., Defoort, S., Ponchel, A., Waucquier, N., Deplanque, D., Deguil, J. & Bordet, R. Donepezil increases contrast sensitivity for the detection of objects in scenes. *Behav. Brain Res.* **292**, 443–447 (2015).

36. Gratton, C., Yousef, S., Aarts, E., Wallace, D. L., D'Esposito, M. & Silver, M. A. Cholinergic, But Not Dopaminergic or Noradrenergic, Enhancement Sharpens Visual Spatial Perception in Humans. *J. Neurosci.* **37**, 4405–4415 (2017).

37. Urai, A. E., Braun, A. & Donner, T. H. Pupil-linked arousal is driven by decision uncertainty and alters serial choice bias. *Nat. Commun.* **8**, 14637 (2017).

38. van Vugt, M. K., Beulen, M. A. & Taatgen, N. A. Relation between centro-parietal positivity and diffusion model parameters in both perceptual and memory-based decision making. *Brain Res.* **1715**, 1–12 (2019).

39. Murphy, P. R., Vandekerckhove, J. & Nieuwenhuis, S. Pupil-Linked Arousal Determines Variability in Perceptual Decision Making. *PLOS Comput. Biol.* **10**, e1003854 (2014).

40. O'Connell, R. G., Dockree, P. M. & Kelly, S. P. A supramodal accumulation-to-bound signal that determines perceptual decisions in humans. *Nat. Neurosci.* **15**, 1729–1735 (2012).

41. Twomey, D. M., Murphy, P. R., Kelly, S. P. & O'Connell, R. G. The classic P300 encodes a build-to-threshold decision variable. *Eur. J. Neurosci.* **42**, 1636–1643 (2015).

42. Kiss, M., Van Velzen, J. & Eimer, M. The N2pc component and its links to attention shifts and spatially selective visual processing. *Psychophysiology* **45**, 240–249 (2008).

43. Di Russo, F., Stella, A., Spitoni, G., Strappini, F., Sdoia, S., Galati, G., Hillyard, S. A., Spinelli, D. & Pitzalis, S. Spatiotemporal brain mapping of spatial attention effects on pattern-reversal ERPs. *Hum. Brain Mapp.* **33**, 1334–1351 (2011).

44. Maris, E. & Oostenveld, R. Nonparametric statistical testing of EEG- and MEG-data. *J. Neurosci. Methods* **164**, 177–190 (2007).

45. Murray, A. M., Nobre, A. C. & Stokes, M. G. Markers of preparatory attention predict visual short-term memory performance. *Neuropsychologia* **49**, 1458–1465 (2011).

46. Praamstra, P. & Kourtis, D. An early parietal ERP component of the frontoparietal system: EDAN not = N2pc. *Brain Res.* **1317**, 203–210 (2010).

47. Capotosto, P., Babiloni, C., Romani, G. L. & Corbetta, M. Frontoparietal Cortex Controls Spatial Attention through Modulation of Anticipatory Alpha Rhythms. *J. Neurosci.* **29**, 5863–5872 (2009).

48. Händel, B. F., Haarmeier, T. & Jensen, O. Alpha Oscillations Correlate with the Successful Inhibition of Unattended Stimuli. *J. Cogn. Neurosci.* **23**, 2494–2502 (2011).

49. Jensen, O. & Mazaheri, A. Shaping Functional Architecture by Oscillatory Alpha Activity: Gating by Inhibition. *Front. Hum. Neurosci.* **4**, 186 (2010).

50. Thut, G. -Band Electroencephalographic Activity over Occipital Cortex Indexes Visuospatial Attention Bias and Predicts Visual Target Detection. *J. Neurosci.* **26**, 9494–9502 (2006).

51. Dahl, M. J., Mather, M. & Werkle-Bergner, M. Noradrenergic modulation of rhythmic neural activity shapes selective attention. *Trends Cogn. Sci.* **26**, 38–52 (2022).

52. Kelly, S. P., Lalor, E. C., Reilly, R. B. & Foxe, J. J. Increases in Alpha Oscillatory Power Reflect an Active Retinotopic Mechanism for Distracter Suppression During Sustained Visuospatial Attention. *J. Neurophysiol.* **95**, 3844–3851 (2006).

53. Ferguson, K. A. & Cardin, J. A. Mechanisms underlying gain modulation in the cortex. *Nat. Rev. Neurosci.* **21**, 80–92 (2020).

54. Gelbard-Sagiv, H., Magidov, E., Sharon, H., Hendler, T. & Nir, Y. Noradrenaline Modulates Visual Perception and Late Visually Evoked Activity. *Curr. Biol.* **28**, 2239-2249.e6 (2018).

55. Kelly, S. P. & O'Connell, R. G. Internal and External Influences on the Rate of Sensory Evidence Accumulation in the Human Brain. *J. Neurosci.* **33**, 19434–19441 (2013).

56. Kanamori, T. & Mrsic-Flogel, T. D. Independent response modulation of visual cortical neurons by attentional and behavioral states. *Neuron* S0896627322008030 (2022) doi:10.1016/j.neuron.2022.08.028.

57. de Gee, J. W., Colizoli, O., Kloosterman, N. A., Knapen, T., Nieuwenhuis, S. & Donner, T. H. Dynamic modulation of decision biases by brainstem arousal systems. *eLife* (2017) doi:10.7554/eLife.23232.

58. Waschke, L., Tune, S. & Obleser, J. Local cortical desynchronization and pupil-linked arousal differentially shape brain states for optimal sensory performance. *eLife* 1–27 (2020) doi:10.1101/582353.

59. de Gee, J. W., Tsetsos, K., Schwabe, L., Urai, A. E., McCormick, D., McGinley, M. J. & Donner, T. H. Pupil-linked phasic arousal predicts a reduction of choice bias across species and decision domains. *eLife* **9**, e54014 (2020).

60. Iemi, L., Busch, N. A., Laudini, A., Haegens, S., Samaha, J., Villringer, A. & Nikulin, V. V. Multiple mechanisms link prestimulus neural oscillations to sensory responses. *eLife* 1–34 (2019) doi:10.1101/461558.

61. Iemi, L. & Busch, N. A. Moment-to-Moment Fluctuations in Neuronal Excitability Bias Subjective Perception Rather than Strategic Decision-Making. *eneuro* **5**, ENEURO.0430-17.2018 (2018).

62. Kloosterman, N. A., de Gee, J. W., Werkle-Bergner, M., Lindenberger, U., Garrett, D. D. & Fahrenfort, J. J. Humans strategically shift decision bias by flexibly adjusting sensory evidence accumulation. *eLife* 1–27 (2019) doi:10.1101/229989.

63. Samaha, J., Iemi, L. & Postle, B. R. Prestimulus alpha-band power biases visual discrimination confidence, but not accuracy. *Conscious. Cogn.* **54**, 47–55 (2017).

64. Zhou, Y. J., Iemi, L., Schoffelen, J.-M., de Lange, F. P. & Haegens, S. Alpha Oscillations Shape Sensory Representation and Perceptual Sensitivity. *J. Neurosci.* **41**, 9581–9592 (2021).

65. Podvalny, E., King, L. E. & He, B. J. Spectral signature and behavioral consequence of spontaneous shifts of pupil-linked arousal in human. *eLife* **10**, e68265 (2021).

66. McGinley, M. J., David, S. V. & McCormick, D. A. Cortical Membrane Potential Signature of Optimal States for Sensory Signal Detection. *Neuron* **87**, 179–192 (2015).

67. Reimer, J., McGinley, M. J., Liu, Y., Rodenkirch, C., Wang, Q., McCormick, D. A. & Tolias, A. S. Pupil fluctuations track rapid changes in adrenergic and cholinergic activity in cortex. *Nat. Commun.* **7**, 13289 (2016).

68. Megemont, M., McBurney-Lin, J. & Yang, H. Pupil diameter is not an accurate real-time readout of locus coeruleus activity. *eLife* **11**, e70510 (2022).

69. Howe, W. M., Gritton, H. J., Lusk, N. A., Roberts, E. A., Hetrick, V. L., Berke, J. D. & Sarter, M. Acetylcholine Release in Prefrontal Cortex Promotes Gamma Oscillations and Theta–Gamma Coupling during Cue Detection. *J. Neurosci.* **37**, 3215–3230 (2017).

70. Parikh, V., Kozak, R., Martinez, V. & Sarter, M. Prefrontal acetylcholine release controls cue detection on multiple timescales. *Neuron* **56**, 141–154 (2007).

71. Knapen, T., de Gee, J. W., Brascamp, J., Nuiten, S., Hoppenbrouwers, S. & Theeuwes, J. Cognitive and Ocular Factors Jointly Determine Pupil Responses under Equiluminance. *PLOS ONE* **11**, e0155574 (2016).

72. VanRullen, R., Busch, N., Drewes, J. & Dubois, J. Ongoing EEG Phase as a Trial-by-Trial Predictor of Perceptual and Attentional Variability. *Front. Psychol.* **2**, (2011).

73. Cicchini, G. M., Benedetto, A. & Burr, D. C. Perceptual history propagates down to early levels of sensory analysis. *Curr. Biol.* **31**, 1245-1250.e2 (2021).

74. Fischer, J. & Whitney, D. Serial dependence in visual perception. *Nat. Neurosci.* **17**, 738–743 (2014).

75. Murphy, P. R., Robertson, I. H., Balsters, J. H. & O'connell, R. G. Pupillometry and P3 index the locus coeruleus–noradrenergic arousal function in humans. *Psychophysiology* **48**, 1532–1543 (2011).

76. Alilović, J., Timmermans, B., Reteig, L. C., van Gaal, S. & Slagter, H. A. No Evidence that Predictions and Attention Modulate the First Feedforward Sweep of Cortical Information Processing. *Cereb. Cortex* **29**, 2261–2278 (2019).

77. Baumgartner, H. M., Graulty, C. J., Hillyard, S. A. & Pitts, M. A. Does spatial attention modulate the earliest component of the visual evoked potential? *Cogn. Neurosci.* **9**, 4–19 (2018).

78. Hillyard, S. A. & Anllo-Vento, L. Event-related brain potentials in the study of visual selective attention. *Proc. Natl. Acad. Sci.* **95**, 781–787 (1998).

79. Nuiten, S. A., Canales-Johnson, A., Beerendonk, L., Nanuashvili, N., Fahrenfort, J. J., Bekinschtein, T. & Gaal, S. van. Preserved sensory processing but hampered conflict detection when stimulus input is task-irrelevant. *eLife* https://elifesciences.org/articles/64431/figures (2021) doi:10.7554/eLife.64431.

80. Silver, M. A., Shenhav, A. & D'Esposito, M. Cholinergic Enhancement Reduces Spatial Spread of Visual Responses in Human Early Visual Cortex. *Neuron* **60**, 904–914 (2008).

81. Knott, V., Choueiry, J., Dort, H., Smith, D., Impey, D., de la Salle, S. & Philippe, T. Baseline-dependent modulating effects of nicotine on voluntary and involuntary attention measured with brain event-related P3 potentials. *Pharmacol. Biochem. Behav.* **122**, 107–117 (2014).

82. Boehler, C. N., Tsotsos, J. K., Schoenfeld, M. A., Heinze, H.-J. & Hopf, J.-M. The Center-Surround Profile of the Focus of Attention Arises from Recurrent Processing in Visual Cortex. *Cereb. Cortex* **19**, 982–991 (2009).

83. Dehaene, S., Changeux, J.-P. & Naccache, L. The Global Neuronal Workspace Model of Conscious Access: From Neuronal Architectures to Clinical Applications. in *Research and Perspectives in Neurosciences* vol. 18 55–84 (2011).

84. Donohue, S. E., Schoenfeld, M. A. & Hopf, J.-M. Parallel fast and slow recurrent cortical processing mediates target and distractor selection in visual search. *Commun. Biol.* **3**, 1–10 (2020).

85. Lamme, V. A. F. & Roelfsema, P. R. The distinct modes of vision offered by feedforward and recurrent processing. *Trends Neurosci.* **23**, 571–579 (2000).

86. Murphy, P. R., Wilming, N., Hernandez-Bocanegra, D. C., Prat-Ortega, G. & Donner, T. H. Adaptive circuit dynamics across human cortex during evidence accumulation in changing environments. *Nat. Neurosci.* **24**, 987–997 (2021).

87. Pereira, M., Perrin, D. & Faivre, N. A leaky evidence accumulation process for perceptual experience. *Trends Cogn. Sci.* **26**, 451–461 (2022).

88. Pitts, M. A., Metzler, S. & Hillyard, S. A. Isolating neural correlates of conscious perception from neural correlates of reporting one's perception. *Front. Psychol.* **5**, 1078 (2014).

89. Seijdel, N., Loke, J., Klundert, R. van de, Meer, M. van der, Quispel, E., Gaal, S. van, Haan, E. H. F. de & Scholte, H. S. On the Necessity of Recurrent Processing during Object Recognition: It Depends on the Need for Scene Segmentation. *J. Neurosci.* **41**, 6281–6289 (2021).

90. Theeuwes, J. Top–down and bottom–up control of visual selection. *Acta Psychol. (Amst.)* **135**, 77–99 (2010).

91. Wang, X.-J. Decision Making in Recurrent Neuronal Circuits. *Neuron* **60**, 215–234 (2008).

92. Ogura, H., Kosasa, T., Kuriya, Y. & Yamanishi, Y. Comparison of inhibitory activities of donepezil and other cholinesterase inhibitors on acetylcholinesterase and butyrylcholinesterase in vitro. *Methods Find. Exp. Clin. Pharmacol.* **22**, 609–613 (2000).

93. Peirce, J. W. PsychoPy--Psychophysics software in Python. *J. Neurosci. Methods* **162**, 8–13 (2007).

94. Posner, M. I. Orienting of attention. *Q. J. Exp. Psychol.* **32**, 3–25 (1980).

95. Kaernbach, C. Simple adaptive testing with the weighted up-down method. *Percept. Psychophys.* **49**, 227–229 (1991).

96. Jas, M., Engemann, D. A., Bekhti, Y., Raimondo, F. & Gramfort, A. Autoreject: Automated artifact rejection for MEG and EEG data. *NeuroImage* **159**, 417–429 (2017).

97. Cohen, M. X. *Analyzing Neural Time Series Data: Theory and Practice*. (MIT Press, 2014).

98. Gramfort, A., Luessi, M., Larson, E., Engemann, D., Strohmeier, D., Brodbeck, C., Goj, R., Jas, M., Brooks, T., Parkkonen, L. & Hämäläinen, M. MEG and EEG data analysis with MNE-Python. *Front. Neurosci.* **7**, 267 (2013).

99. Norris, H. The action of sedatives on brain stem oculomotor systems in man. *Neuropharmacology* **10**, 181–191 (1971).

100. Bond, A. & Lader, M. The use of analogue scales in rating subjective feelings. *Br. J. Med. Psychol.* **47**, 211–218 (1974).

101. JASP TEAM. JASP. (2022).

102. Wiecki, T., Sofer, I. & Frank, M. HDDM: Hierarchical Bayesian estimation of the Drift-Diffusion Model in Python. *Front. Neuroinformatics* **7**, (2013).